CRISPR/Cas9-mediated Base-editing Enables a Chain Reaction Through Sequential Repair of sgRNA Scaffold Mutations

Tsuyoshi Fukushima
The Institute of Medical Science, The University of Tokyo
Yosuke Tanaka
The Institute of Medical Science, The University of Tokyo
Keito Adachi
The Institute of Medical Science, The University of Tokyo
Nanami Masuyama
University of Tokyo
Shuhei Asada
The Institute of Medical Science, The University of Tokyo
Soh Ishiguro
University of Tokyo
Hideto Mori
University of Tokyo
Motoaki Seki
University of Tokyo
Nozomu Yachie
University of Tokyo
Susumu Goyama
The Institute of Medical Science, The University of Tokyo
Toshio Kitamura (kitamura@ims.u-tokyo.ac.jp)
The Institute of Medical Science, The University of Tokyo

Research Article

Keywords: Cellular behavior, cytosine nucleotide deaminase, thymidine (T)-to-cytosine (C) substitutions

Posted Date: February 19th, 2021

DOI: https://doi.org/10.21203/rs.3.rs-199062/v1

Version of Record: A version of this preprint was published at Scientific Reports on December 1st, 2021.
See the published version at https://doi.org/10.1038/s41598-021-02986-6.

Abstract

Cellular behavior is governed by the complex gene regulatory networks. Although studies have revealed diverse roles of individual genes, it has been a challenge to record or control the sequential genetic events in living cells. In this study, we designed two cellular chain reaction systems that enable sequential sgRNA expression in mammalian cells using a nickase Cas9 tethering of a cytosine nucleotide deaminase (nCas9-CDA). In these systems, the thymidine (T)-to-cytosine (C) substitutions in the scaffold region of sgRNA or TATA box containing loxP sequence (TATAloxP) are corrected by the nCas9-CDA, which leads to expression of next sgRNA. These reactions can proceed several times, thus generating cellular chain reactions. As a proof of the concept, we established a chain reaction through the repair of sgRNA scaffold mutations in 293T cells. Importantly, the results obtained in yeast or *in vitro* were not consistent with those in mammalian cells, suggesting that the *in vivo* chain reactions need to be optimized in appropriate cellular contexts. Our system may lay the foundation for building cellular chain reaction systems that have a broad utility in the future biomedical research.

Introduction

A chain reaction is a sequence of related events or reactions in which each event/reaction causes the next one. Because many biological processes are composed of sequential chemical or cellular reactions, methods and platforms that enable molecular recording or intervention of the sequential events in living cells have broad applications in the field of cell biology, bioengineering and therapeutics.

Several systems to record chain reactions have been developed in mammalian cells. *Friedland et al* generated two cellular chain reaction systems using T7/T3 RNA-polymerases and Cre/Flippase (Flp) recombinases. In the former system, T7 RNA-polymerase induced expression of T3 RNA-polymerase and then T3 RNA-polymerase induced next reaction[1]. In the latter system, recombination of flippase recognition target (FRT) by Flp induced Cre expression and then Cre-induced loxP recombination induced next reaction. Because the numbers of RNA-polymerases and recombinases are limited, the number of chain reactions is limited in these systems. More recently, *Farzadfard et al* generated an elegant chain reaction system, called DOMINO[2], using a nickase Cas9 tethering of a cytosine nucleotide deaminase (nCas9-CDA) that induces efficient substitution of cytosine nucleotide (C) to thymidine nucleotide (T) in the genomic sequence[3]. In the DOMINO system, the C>T modification in target DNA locus by sgRNA and nCas9-CDA provoked next modification. *Farzadfard et al* also achieved conversion of inactive sgRNA to active sgRNA by introducing C>T substitutions in the protospacer sequence of nonfunctional sgRNA. One limitation of this system is the difficulty of generating multiple active sgRNAs during chain reactions because the protospacer sequence is strictly dependent on the sequence of target DNA.

To establish platforms that enable sequential activation of multiple sgRNAs, we designed two nCas9-CDA-based chain reaction systems through sequential repair of mutations in sgRNA scaffold or TATAloxP sequences. We generated several PAM-inserted sgRNAs without loss of function and successfully inactivated them by introducing T>C mutations that can be repaired by nCas9-CDA. As a proof of the

concept, we established a cellular chain reaction through the repair of sgRNA scaffold mutations in 293T cells. Our system may lay the foundation for building sophisticated chain reaction systems in living cells.

Results

Two strategies to generate cellular chain reactions using nCas9-CDA

We designed two systems to generate chain reactions using nCas9-CDA. In the first system, the T>C mutations are introduced in the scaffold region of sgRNA to disrupt its structure. The T>C mutations in the sgRNA (sgRNA-2) are corrected by nCas9-CDA and another sgRNA (sgRNA-1). The corrected sgRNA-2 in turn corrects the T>C mutations in the third sgRNA (sgRNA-3) in cooperation with nCas9-CDA (Fig. 1A). Because the sequence and the length of the stem-loop region in the sgRNA scaffold are not restrictive[4,5], we can design multiple sgRNAs by introducing various sequences in the stem-loop region (XXXXX in sgRNA-2-MT, YYYYY in sgRNA-3-MT) (Fig. 1B).

In the second system, the T>C mutations are introduced in the TATAloxP sequence (TATAloxP-MT). TATAloxP forms a 13-8-13 structure, which is composed of an 8-bp spacer sequence containing TATA box flanked on either side by two 13-bp inverted repeats (Fig. 1C). Cre recombinase binds to the 13 bp repeats of the TATAloxP, and importantly, this TATA box containing sequence can be incorporated into the U6 promoter to induce sgRNA expression[6]. The T>C mutations in the TATAloxP are corrected by the nCas9-CDA and the sgRNA (sgRNA-1) targeting the mutations and adjacent sequences (XXXXX in Fig. 1D). After the correction, a loxP flanked stop cassette is excised by Cre recombinase, which drives expression of the second sgRNA (sgRNA-2). The sgRNA-2 targets the next mutatiosn and adjacent sequences (YYYYY in Fig. 1D), resulting in expression of the third sgRNA (sgRNA-3) (Fig. 1D). Because there is no restriction for the adjacent sequences, we can design multiple sgRNAs with various adjacent sequences that can be activated during the chain reaction.

Generation of inactive sgRNAs with T>C mutations in the scaffold region

To establish the first system, we introduced T>C mutations in the template sequence of the sgRNA scaffold region for its inactivation. Because nCas9-CDA was shown to induce C>T substitution in DNA efficiently when the cytosine is located 18bp upstream from PAM sequence[3], we also introduced PAM sequence (NGG) 18 bp downstream from the T>C mutation in each sgRNA template (Fig. 2A and 2B). We then assessed activity of each sgRNA with the T>C mutations and PAM insertion using canavanine assay. Canavanine is a toxic analogue of arginine and is imported into yeast cells via a transporter Can1. Therefore, expression of Cas9 and *Can1*-targeting sgRNA induces Can1 depletion and decreases the sensitivity of yeast to canavanine[7]. We used this assay to evaluate impact of each T>C mutation for inactivation of the sgRNA, and found that the T>C mutation at 4th base resulted in sgRNA inactivation in yeast. Insertion of PAM sequence did not inhibit the sgRNA function in yeast (Fig. 2D and 2E).

We then assessed the effect of the T>C mutations on sgRNA function in mammalian cells. Mutant EGFP in which the start codon was mutated from ATG to GTG was used[8]. In this mutant EGFP, the template strand has a T>C mutation at start codon and its 18bp-downstream PAM sequence. Therefore, expression of nCas9-CDA and active sgRNA can correct the T>C mutation in the mutant EGFP to induce GFP expression (Fig. 3A and 3B). Unfortunately, unlike the results obtained by the canavanine assay, insertion of PAM sequence itself inactivated sgRNA in mammalian cells (Fig. 3C). Because the weak interaction between G and U is known to be important for maintaining RNA structure[9], we speculated that the loss of G-U interaction at 7th base induced by the PAM insertion might impair sgRNA function (Fig. 3D). Therefore, we introduced additional sequences near to the PAM sequence to maintain the G-U interaction at 7th base. Elongation of the stem-loop sequences in the sgRNA scaffold was shown to have little influence on sgRNA function[4,5]. As expected, this optimized PAM-inserted sgRNA retained the G-U interaction at 7th base (Fig. 3D) and efficiently induced GFP expression when it was expressed with nCas9-CDA and mutant EGFP in 293T cells (Fig. 3E).

We next examined if the T>C mutation at 4th base, which diminished sgRNA activity in yeast, also inactivates sgRNA in mammalian cells. Again, we got different results in mammalian cells from those obtained by the canavanine assay. The sgRNA with single T>C mutation at 4th base efficiently induced GFP expression, suggesting that it retained normal function. Therefore, we introduced T>C mutations at 2, 3, or 5th base to the sgRNA template in addition to the 4th base. These sgRNAs with double T>C mutations at 2/4th, 3/4th, 4/5th bases lost the function to recover GFP expression in 293T cells (Fig. 3F). We then performed similar experiments using the PAM-inserted sgRNAs and confirmed that the double T>C mutations at 3/4th bases, but not single T>C mutation at 4th base, resulted in loss of sgRNA function (Fig. 3G). Thus, we generated an inactive sgRNA with T>C mutations and PAM sequence in the scaffold region, whose function can theoretically be recovered by the nCas9-CDA-induced base editing in mammalian cells.

Generation of non-responsive TATAloxP sequences with T>C mutations

To establish the second system, we introduced T>C mutations in the TATAloxP sequences to make it non-responsive to Cre-induced recombination. We generated several TATAloxP mutants in which one base of C in the 13 bp repeat sequence (Fig. 1C) was replaced with T. These DNAs with various TATAloxP sequences at either 5' or 3' sides (approximately 3500 bp) were linearized and incubated with Cre recombinase. In this *in vitro* assay, Cre-induced recombination produces approximately 7000 bp linear DNA when the Cre recombinase can recognize the TATAloxP sites (Fig. 4A). As shown in Fig. 4B and 4C, the T>C mutation at the 13th base resulted in the reduced recombination in both mutant/mutant and mutant/wild-type incubations.

Next, we examined if the TATAloxP sequences with the T>C mutations are resistant to Cre-mediated recombination in mammalian cells. We generated an expression vector containing polyA signal flanked with two TATAloxP sites and a downstream EGFP cassette under EF1a promoter, in which one of the

TATAloxP site has the T>C mutations. If the mutant TATAloxP site is resistant to Cre-mediated recombination, GFP is not expressed even in the presence of Cre-recombinase (Fig. 4D). We expressed the TATAloxP (wild-type or mutant)-EGFP constructs in 293T cells together with Cre-R32V, a mutant Cre recombinase with improved accuracy[10] (Fig. 4E). However, unlike the results of *in vitro* experiments, the T>C mutation at the 13th base in one or both 13-bp arms did not prevent Cre-R32V-induced GFP expression (Fig. 4F). Thus, the T>C mutation at 13th base was not sufficient to make the TATAloxP sequence non-responsive to Cre recombinase in mammalian cells. Because a previous report showed that double mutations in the both 13-bp arms, in particular at the 7th, 8th, 11th, 12th and 13th base, disrupt loxP structure efficiently[11], we then assessed the effect of double T>C mutations at 11th and/or 13th base on their responsiveness to Cre recombinase. Among the various combinations, we found that double T>C mutations at 11th and 13th bases in both arms became resistant to Cre-induced GFP expression (Fig. 4G). Thus, we generated a non-responsive TATAloxP sequence with T>C mutations, whose responsiveness to Cre can theoretically be recovered by the nCas9-CDA-induced base editing in mammalian cells.

Establishment of a chain reaction in mammalian cells

Finally, we examined whether the inactive sgRNA or the non-responsive TATAloxP with T>C mutations can be converted to the active form by the nCas9-CDA-induced base editing in mammalian cells. First, we transduced nCas9-CDA, the mutant EGFP, PAM-inserted control or inactive sgRNA targeting the EGFP mutation with or without the second sgRNA into 293T cells. The second sgRNA was designed to correct the T>C mutations in the EGFP-targeting sgRNA to make it an active form (Fig. 5A and 5B). As expected, the optimized version of PAM-inserted sgRNA efficiently corrected the EGFP mutation and induced GFP expression, while that with T>C mutation did not. Importantly, coexpression of the second sgRNA recovered the function of the inactive sgRNA to drive robust GFP expression in 293T cells (Fig.5C). Thus, the chain reaction was successfully achieved in mammalian cells using nCas9-CDA and two sgRNAs targeting the T>C mutation or EGFP mutation.

Second, we transduced wild-type and the non-responsive TATAloxP-EGFP, Cre-R32V and nCas9-CDA with or without the second sgRNA into 293T cells. The second sgRNA was designed to correct the T>C mutations in the non-responsive TATAloxP to convert it to a responsive form (Fig. 5D and 5E). Consistent with earlier results, Cre-R32V induced recombination of only wild-type TATAloxP, but not mutant TATAloxP, to induce GFP expression in 293T cells (Fig. 5F). Unfortunately, coexpression of the second sgRNA did not recover the GFP expression, indicating that the mutant TATAloxP with double T>C mutations at 11th and 13th bases is resistant to the nCas9-DNA-mediated base editing. Thus, this TATAloxP system is not suitable for cellular chain reactions in its current form.

Discussion

To generate the system enabling sequential sgRNA activation in mammalian cells, we designed two chain reaction systems using the nCas9-CDA base editor. As a proof of the concept, we successfully established a chain reaction through the repair of sgRNA scaffold mutations in 293T cells. In our system,

there is no theoretical limit on the number of times for sequential reactions. Furthermore, our system allows activation of different sgRNAs in each stage of chain reaction. Thus, our chain reaction system will provide a useful platform to record and control molecular events in living cells. For example, the chain reaction system combined with the DNA barcoding technique will enable sequential cellular barcoding to understand individual cell fates with DNA memory. It will also be interesting to combine the cell cycle-dependent CRISPR-Cas9 activation system[12] with our chain reaction system to develop the counter of cell division. With such technology, we will be able to determine how many times the cell has divided from stem cells in future studies.

However, further optimization will be required to develop more sophisticated chain reaction systems in mammalian cells. Although we achieved the chain reaction using the sgRNA scaffold mutation system, the activity of the repaired sgRNA was much weaker than the control sgRNA. We could not even recover the responsiveness of the mutant TATAloxP by the nCas9-CDA-mediated base editing in mammalian cells. To achieve more robust chain reactions, it is necessary to increase the repair rate of the mutation in each step. Our study also revealed that the results obtained in yeast or *in vitro* were not consistent with those in mammalian cells. It has been shown that physiological RNA structure depends not only on sequence but also on RNA-modifications and binding proteins[13]. It was also shown that DNA methylation affects the efficiency of Cre-mediated recombination[14]. These *in vivo* specific regulatory mechanisms could explain the discrepancy between the *in vitro* and *in vivo* results. Thus, our findings strongly indicate that the *in vivo* chain reactions need to be optimized in appropriate cellular contexts.

In summary, we established a cellular chain reaction system using the nCas9-CDA mediated base-editing of sgRNA scaffold mutations. Our system combined with tissue specific or time-dependent regulation may have a broad utility in future biomedical research.

Methods

Plasmids

Plasmids and primers used for plasmid construction are summarized in Supplemental Table 1. Mutations were introduced by PCR using KOD FX NEO (TOYOBO), and the mutants were cloned into vectors using Gibson assembly using Gibson Assembly Master Mix (NEB). TATAloxP sequence was generated using gBlocks (IDT). For plasmid construction of pNMA001, the gRNA encoding region were amplified by PCR using primers (5’-GTTTTAGAGCTAGAAATAGCAAGTTAAAATA

AGGCTAGTCCGTTATCAACTTGAAAAAGTGGCACCGAGTCGGTGGTGCTTTTTT GTTCAC

TGCCGTATAGGCAG-3’ and 5’-AAACTTCTCCGCAGTGAAAGATAAATGATCGTCAATTACG

AAGACTGAACGTTTTAGAGCTAGAAATAGC-3’). The amplified product and p426-SNR52p-gRNA.CAN1.Y-SUP4t (Addgene#43803) backbone fragment amplified by PCR using primers (5’-GATCATTTATCTTTCACTGCGG-3’ and 5’-TGTTTTTTATGTCTTCGAGTCATGTAATTA-3’ were then

assembled by Gibson Assembly. For plasmid construction of pLV-U6p-gRNA-CMVp-nCas9-PmCDA1-UGI-2A-mCherry, the human U6 promoter and gRNA encoding region were amplified by PCR from pSI-236 plasmid using primers (5'-GGGACAGCAGAGATCCAGTTTATCG

ATGAGGGCCTATTTCCCATG-3') and (5'-GTAATTGATTACTATTAATAACTAGTAAAAAAGC

ACCGACTC GGT-3'). The amplified product and pLV-CS-086 backbone fragment digested by SpeI and ClaI were then assembled by Gibson Assembly.

Cell Culture

293T cells were cultured in DMEM (Wako) containing 10% fetal bovine serum (FBS) (biowest) at 37℃ with 5% CO_2. 293T was authenticated by short-tandem repeat analyses and tested for mycoplasma contamination in our laboratory. One mg/ml of puromycin (Thermo Fisher Scientific), 5 mg/ml of Blasticidin S (Thermo Fisher Scientific) and 1 mg/ml of Zeosin (InvivoGen) were used for selection.

Transient Transfection

Plasmids were transfected using the calcium-phosphate coprecipitation method[15]. Mixture of 10-20 ng plasmid (10-20 ml), 2.5 M $CaCl_2$ (50 ml) and filtered water (430-440 ml) to 2×HeBS (500 ml) was added to 293T cells in a 10 cm dish (2.0×10^6 cells/dish) for 18 hours. For integration of Piggyback vector, 15 mg of Piggyback vector and 5 mg of pLG2 (PB200PA-1, SBI) were co-transfected with the above-mentioned plasmids.

Viral Transduction

Lentiviruses and retroviruses were produced by transient transfection in 293T cells using the calcium-phosphate method, as described above. Mixture of plasmids (3 ng of VSVG and 10 ng of PAX2 for lentivirus, 3 mg of RD114 and 10 mg of M57 for retrovirus together with 12 mg virus vectors), 2.5 M $CaCl_2$ (50 ml) and filtered water (425 ml) to 2×HeBS (500 ml) was added to 293T cells in a 10 cm dish (2.0×10^6 cells/dish). After 24 hours, we removed medium by aspiration and added 5 ml of fresh DMEM(Wako)/10% FBS (biowest). Virus-containing medium was collected 48 hours after the transfection.

In vitro Cre recombinase reaction assay

One mg of mutant TATAloxP sequences in Zero-blant vector (Thermo Fisher Scientific) were incubated with 1.5 U/ml BamH□, 1.0 U/ml Not□ or 1.0 U/ml Mlu□ to linearize them. The linear DNAs (20 ng each) were mixed with 10x Cre Recombinase Reaction Buffer, Cre Recombinase, and H_2O and were incubated at 37°C for 30 minutes and then 70°C for 10 minutes.

Live cell imaging

Live-cell imaging was performed using the Invitrogen EVOS FL Auto 2 Imaging System (Thermo Fisher Scientific). Phase contrast images were acquired using a 10x phase contrast objective and a camera (at 1388x1040 pixel resolution). EGFP images were acquired using the EVOS^{TM} LED Cube, GFP.

Flowcytometry analysis

293T cells were resuspended with PBS containing 2% FBS. Cells were then analyzed on a FACS Verse (BD Biosciences).

Canavanine assay

The Saccharomyces cerevisiae strain BY4741 (MATa his3D0leu2D0 met15D0 ura3D0) was used in the CAN1 mutagenesis analysis of the CRISPR system. Parental BY4741 were grown in YPAD before transformation and then propagated in the appropriate synthetic complete (SC) media minus the auxotrophic compound complemented by the plasmids. BY4741 were spread to YPAD plate at day 1. At day 3, BY4741 single colony were picked and cultured in 5 ml YPAD at 30℃ overnight. At day 4, transformation of plasmids harboring galactose-inducible modifier gene plasmid (Cas9, nCas9-CDA) containing LEU2 marker and gRNA-expressing plasmid containing Ura3 marker (each 250 mg per transformation) was carried out using a Frozen EZ Yeast transformation Kit (ZYMO RESEARCH). After transformation, BY4741 were spread to SC-Leu-Ura+Ade plates for selection. At day 6, single colony from each plate were picked and cultured in 5 ml SC-Leu-Ura-Ade at 30℃. Culture media was changed to SRaffi-Leu-Ura+Ade at day8. Culture media was changed to SGall-Leu-Ura+Ade at day10. At day11, BY4741 were spread to SC-Leu-Ura+Ade+canavanine plates or SC-Leu-Ura+Ade plates.

Declarations

Data availability

Information and requests for reagents may be directed to the lead contact Yosuke Tanaka (ytims@ims.u-tokyo.ac.jp).

Acknowledgments

We thank the Flow Cytometry Core at The Institute of Medical Science, The University of Tokyo for their help. This project was supported by “Grant-in-Aid for Challenging Exploratory Research” from JSPS to Y.T. (19K22380) and “Grant-in-Aid for Challenging Exploratory Research” from JSPS to Tsu.F. (20K21613).

Author contributions

Tsu.F. and Y.T. designed most of the experiments. Tsu.F. and K.A. performed most of the experiments. N.M performed canavanine assay. S.A., S.I., H.M. and M.S. supported to design the experiments. Tsu.F., S.G., S.A. and T.K. wrote the manuscript. Y.T, T.K. Y.N. and S.G. supervised and coordinated the project.

References

1 Friedland, A. E. *et al.* Synthetic gene networks that count. *Science***324**, 1199-1202, doi:10.1126/science.1172005 (2009).

2 Farzadfard, F. *et al.* Single-Nucleotide-Resolution Computing and Memory in Living Cells. *Mol Cell***75**, 769-780.e764, doi:10.1016/j.molcel.2019.07.011 (2019).

3 Nishida, K. *et al.* Targeted nucleotide editing using hybrid prokaryotic and vertebrate adaptive immune systems. *Science***353**, doi:10.1126/science.aaf8729 (2016).

4 Chen, B. *et al.* Dynamic imaging of genomic loci in living human cells by an optimized CRISPR/Cas system. *Cell***155**, 1479-1491, doi:10.1016/j.cell.2013.12.001 (2013).

5 Nishimasu, H. *et al.* Crystal structure of Cas9 in complex with guide RNA and target DNA. *Cell***156**, 935-949, doi:10.1016/j.cell.2014.02.001 (2014).

6 Ventura, A. *et al.* Cre-lox-regulated conditional RNA interference from transgenes. *Proc Natl Acad Sci U S A***101**, 10380-10385, doi:10.1073/pnas.0403954101 (2004).

7 DiCarlo, J. E. *et al.* Genome engineering in Saccharomyces cerevisiae using CRISPR-Cas systems. *Nucleic Acids Res***41**, 4336-4343, doi:10.1093/nar/gkt135 (2013).

8 Sakata, R. C. *et al.* Base editors for simultaneous introduction of C-to-T and A-to-G mutations. *Nat Biotechnol***38**, 865-869, doi:10.1038/s41587-020-0509-0 (2020).

9 Varani, G. & McClain, W. H. The G x U wobble base pair. A fundamental building block of RNA structure crucial to RNA function in diverse biological systems. *EMBO Rep***1**, 18-23, doi:10.1093/embo-reports/kvd001 (2000).

10 Eroshenko, N. & Church, G. M. Mutants of Cre recombinase with improved accuracy. *Nat Commun***4**, 2509, doi:10.1038/ncomms3509 (2013).

11 Hartung, M. & Kisters-Woike, B. Cre mutants with altered DNA binding properties. *J Biol Chem***273**, 22884-22891, doi:10.1074/jbc.273.36.22884 (1998).

12 Matsumoto, D., Tamamura, H. & Nomura, W. A cell cycle-dependent CRISPR-Cas9 activation system based on an anti-CRISPR protein shows improved genome editing accuracy. *Commun Biol***3**, 601, doi:10.1038/s42003-020-01340-2 (2020).

13 Spitale, R. C. *et al.* Structural imprints in vivo decode RNA regulatory mechanisms. *Nature***519**, 486-490, doi:10.1038/nature14263 (2015).

14 Rassoulzadegan, M., Magliano, M. & Cuzin, F. Transvection effects involving DNA methylation during meiosis in the mouse. *Embo j***21**, 440-450, doi:10.1093/emboj/21.3.440 (2002).

15 Kitamura, T. *et al.* Retrovirus-mediated gene transfer and expression cloning: powerful tools in functional genomics. *Exp Hematol***31**, 1007-1014 (2003).

Figures

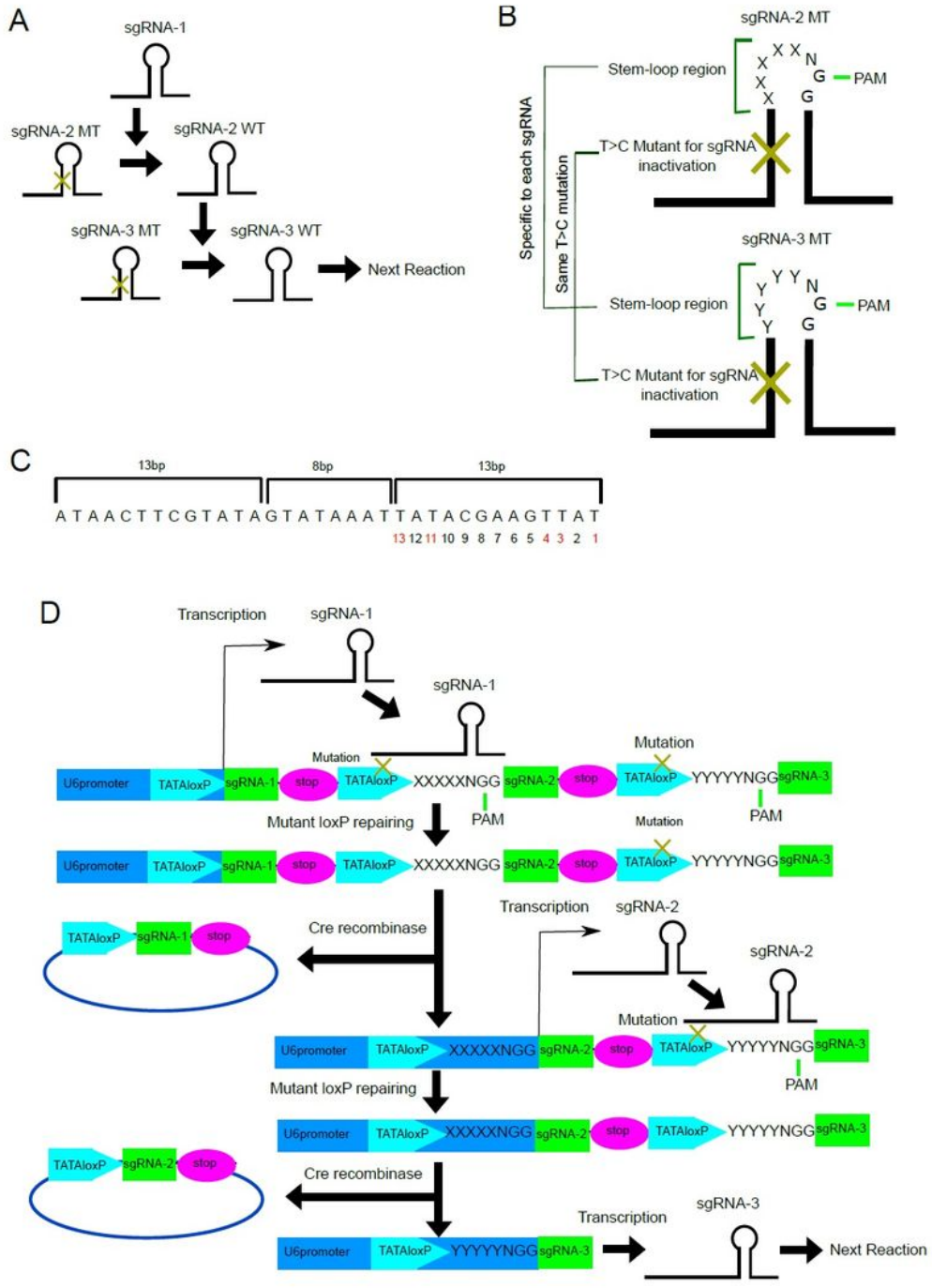

Figure 1

Two strategies to generate chain reactions using nCas9-CDA. (A) Schematic illustration of the chain reaction using nCas9-CDA and sgRNAs with scaffold mutations. (B) Schematic illustration of sgRNA structure with the T>C mutation and specific sequences in the stem-loop region. (C) Schematic illustration of TATAloxP structure and sequences. (D) Schematic illustration of the chain reaction using nCas9-CDA and TATAloxP with T>C mutations.

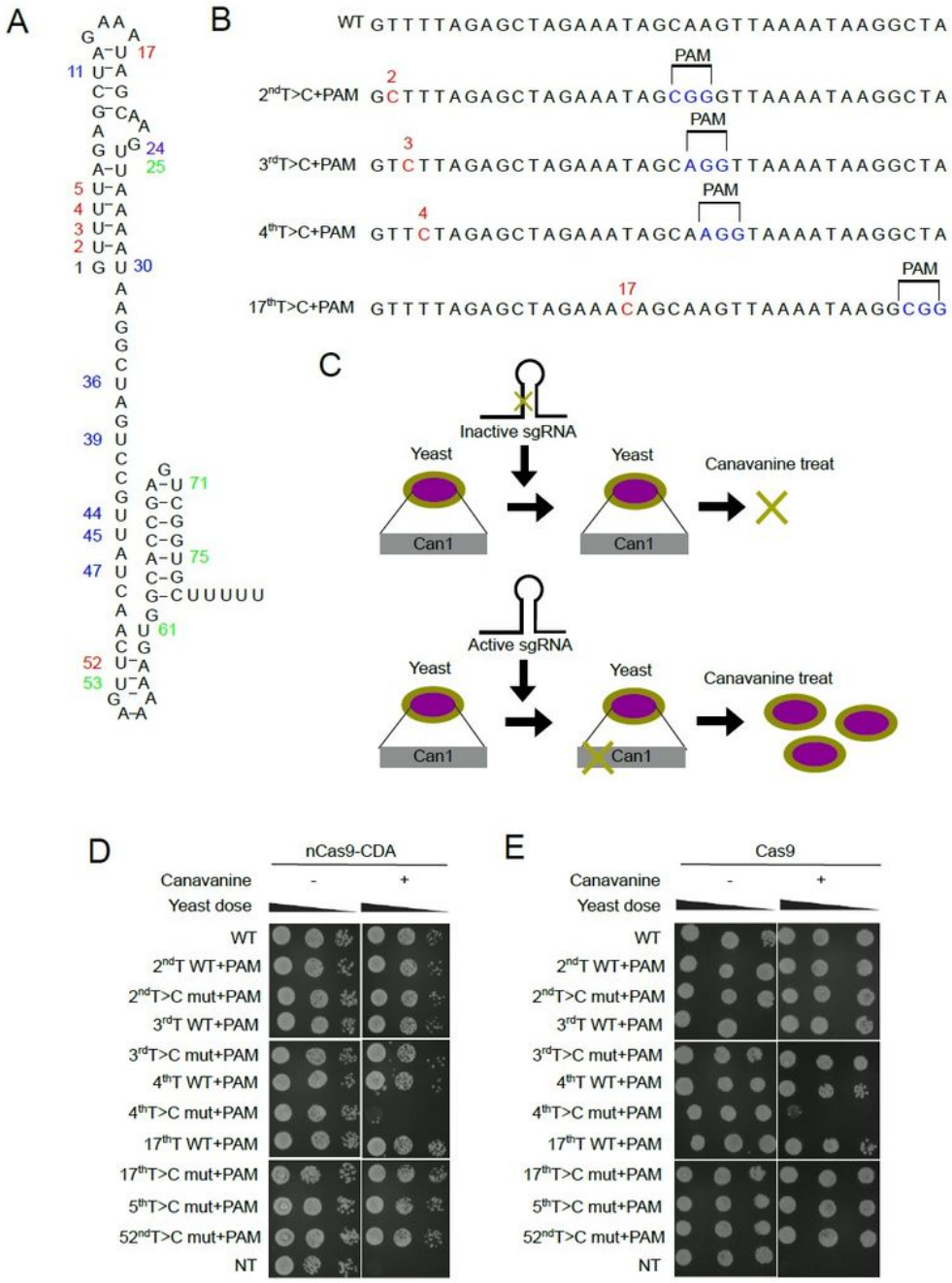

Figure 2

Screening of inactive sgRNAs with scaffold mutations in yeast. (A) Schematic illustration of sgRNA scaffold structure. Note that uracil (U) replaces thymine (T) in sgRNA. (B) Schematic illustration of template DNA for the mutant sgRNAs with T>C mutations and PAM insertion in the scaffold region. (C-E) Schematic illustration (C) and results of canavanine assay using nCas9-CDA (D) or Cas9 (E). Yeasts transduced with the indicated sgRNA were grown on plates with (right column) or without (left column) canavanine.

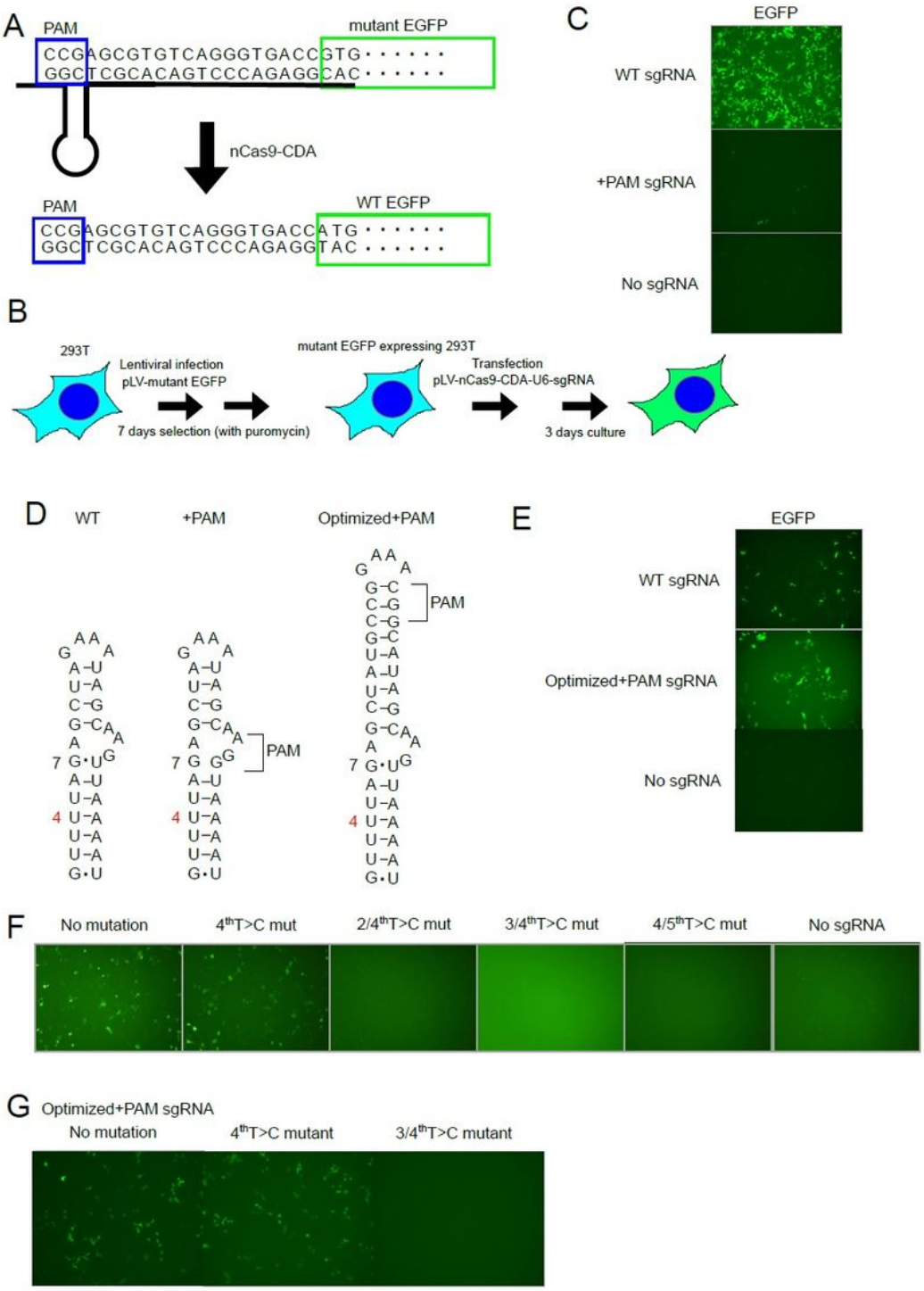

Figure 3

Screening of inactive sgRNAs with scaffold mutations in mammalian cells. (A) Schematic illustration of wild-type and mutant (ATG to GTG) EGFP with PAM sequence insertion. (B) Experimental scheme used in Figure 3C, E-G. 293T cells were transduced with the mutant EGFP. The mutant EGFP-expressing 293T cells were then transfected with nCas9-CDA and sgRNAs targeting the T>C mutation. (C) Fluorescence images of 293T cells expressing mutant EGFP and nCas9-CDA together with wild-type (upper), PAM-inserted (middle) or no (bottom) sgRNA. (D) Schematic illustration of wild-type sgRNA (left) and PAM-inserted sgRNAs (original version: middle, optimized version: right). Note that the G-U interaction at 7th base was lost in the original PAM-inserted sgRNA. The optimized version of PAM-inserted sgRNA contains additional sequences in the stem-loop region to retain the G-U interaction at 7th base. (E) Fluorescence images of 293T cells expressing mutant EGFP and nCas9-CDA together with wild-type (upper), PAM-inserted (middle) or no (bottom) sgRNA. (F, G) Fluorescence images of 293T cells expressing mutant EGFP and nCas9-CDA together with various sgRNAs. The indicated T>C mutations were introduced into the control sgRNA (F) or the optimized PAM-inserted sgRNA (G). mut; mutation.

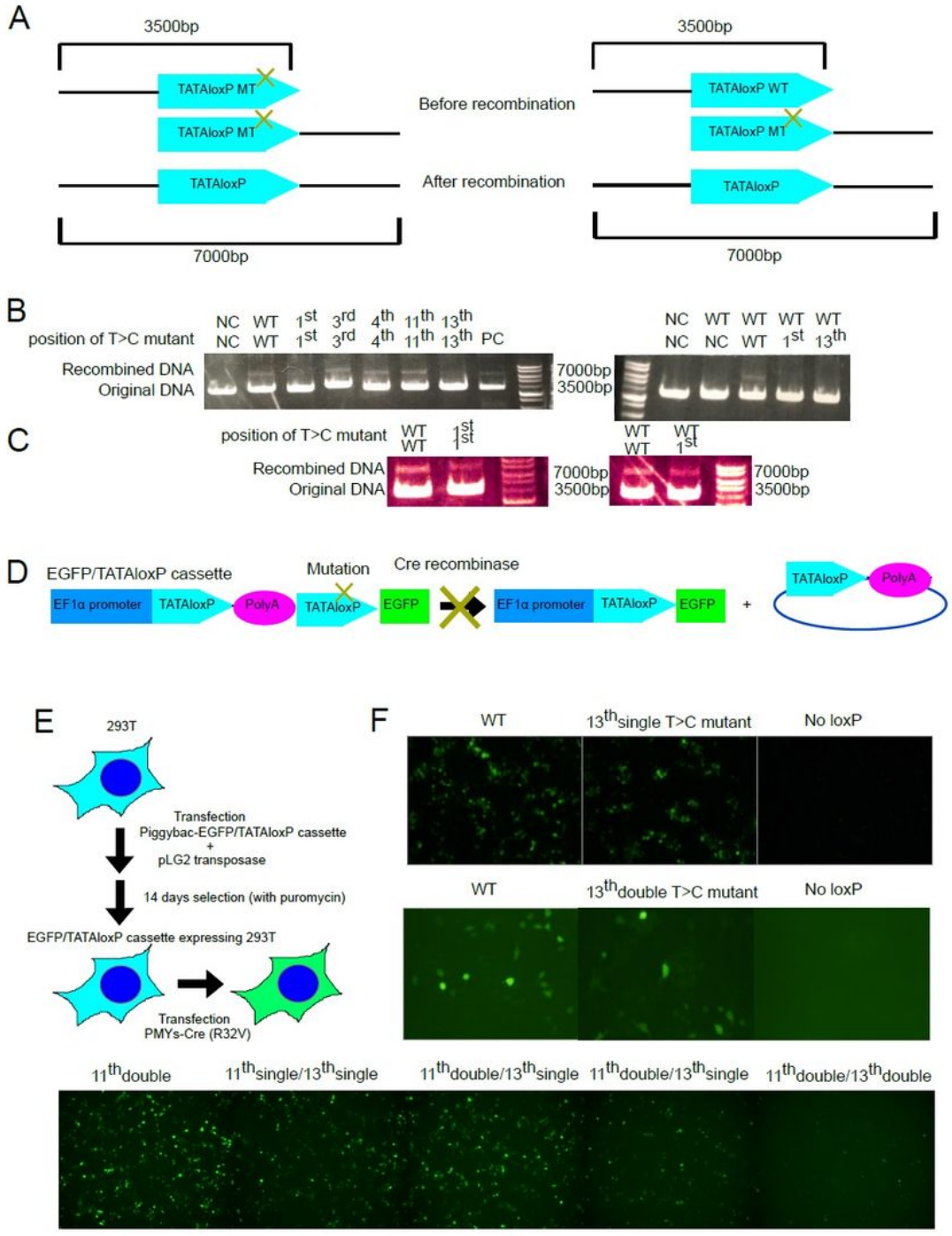

Figure 4

Screening of non-responsive TATAloxP with T>C mutations. (A) Schematic illustration of in vitro recombination assay with TATAloxP sequences with T>C mutations. (B, C) Linear DNAs with various TATAloxP sequences containing the indicated mutations were incubated with Cre recombinase. Note that TATAloxP with T>C mutation at 1st base did not efficiently produce recombined DNA in the initial experiment probably due to technical errors (B), but did produce recombined DNA in the second

experiment (C). (NC; No loxP, PC; Gibson Assembly Positive Control in Gibson Assembly Master Mix) (D) Schematic illustration of EGFP cassette containing mutant TATAloxP and PolyA sequences under EF1α promoter. (E) Experimental scheme used in Fig. 4F. 293T cells were transduced with the EGFP/TATAloxP cassette, and the mutant EGFP-expressing 293T cells were then transfected with nCas9-CDA, Cre-R32V and the indicated sgRNAs. (F) Fluorescence images of 293T cells expressing the EGFP/TATAloxP, nCas9-CDA, Cre-R32V together with various sgRNAs with the indicated T>C mutations. WT; wild-type.

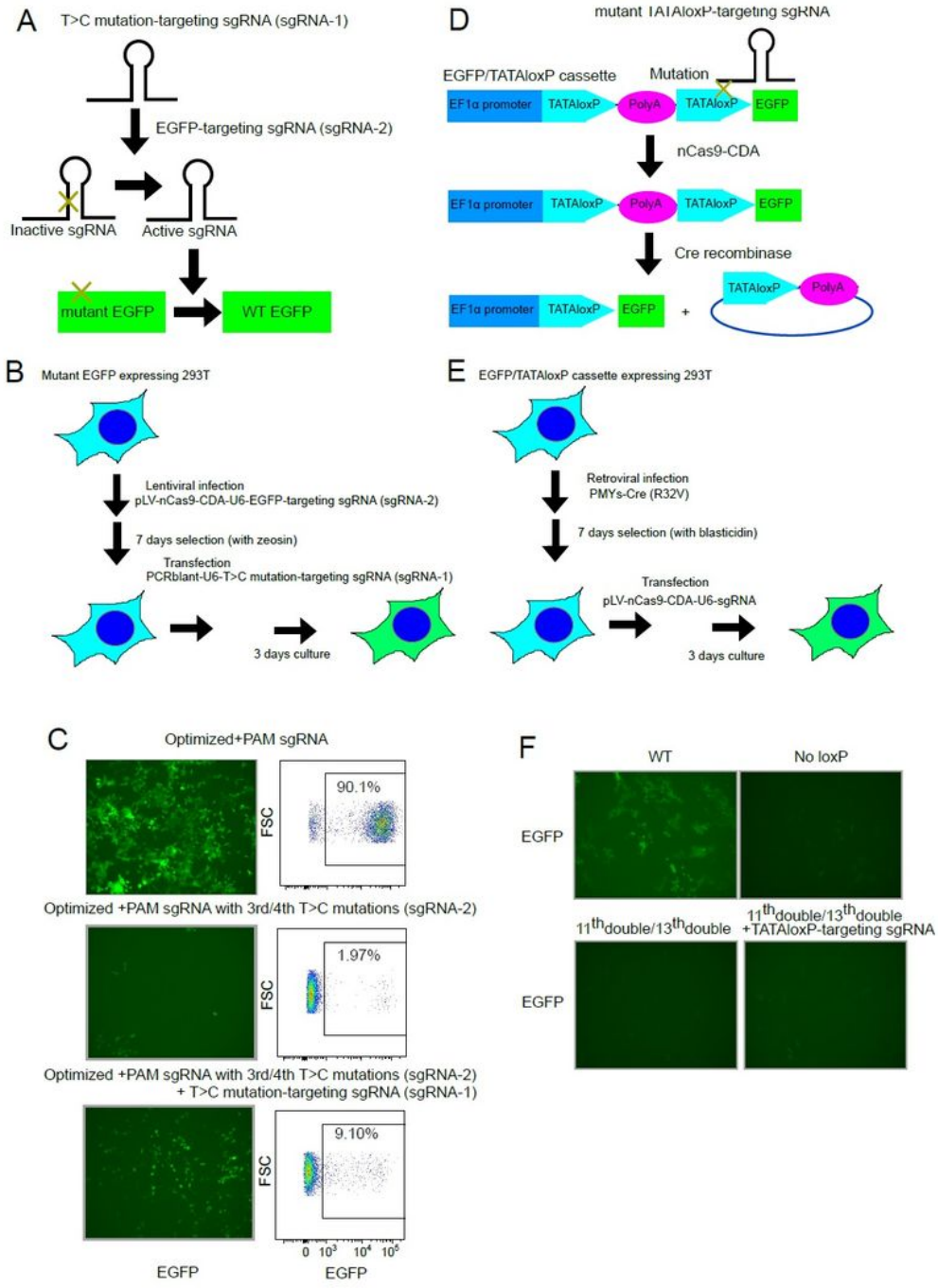

Figure 5

Cellular chain reaction systems using nCas9-CDA. (A) Schematic illustration of the chain reaction through repair of sgRNA scaffold mutations to express GFP in 293T cells. (B) Experimental scheme used in Fig. 5C. 293T cells were transduced with mutant EGFP, and were then transfected with nCas9-CDA, an EGFP-targeting sgRNA, and another sgRNA targeting the T>C mutation. (C) Fluorescence images (left) and FACS plots (right) of 293T cells expressing mutant EGFP and nCas9-CDA together with the indicated sgRNAs. The sgRNA-1 converted the inactive sgRNA-2 to active form, and the sgRNA-2 corrected the EGFP mutation to induce GFP expression. (D) Schematic illustration of the chain reaction through repair of TATAloxP mutations to express GFP in 293T cells. (E) Experimental scheme used in Fig. 5F. 293T cells were transduced with the EGFP/TATAloxP cassette, and were then transfected with nCas9-CDA, Cre-R32V, and the sgRNA targeting the T>C mutation. (F) Fluorescence images of 293T cells expressing EGFP/TATAloxP cassette and nCas9-CDA together with the indicated sgRNAs. No GFP expression was detected when we used the EGFP/TATAloxP cassette with T>C mutations at 11th and 13th bases in both arms even in the presence of the TATAloxP-targeting sgRNA (bottom-right).

Supplementary Files

This is a list of supplementary files associated with this preprint. Click to download.

- supcom.pdf